



## PV-HYBRID AND THERMOELECTRIC COLLECTORS

GUNTER ROCKENDORF<sup>\*†</sup>, ROLAND SILLMANN\*, LARS PODLOWSKI\*\* and  
BERND LITZENBURGER\*\*

\*Institut für Solarenergieforschung GmbH, Hameln/Emmerthal (ISFH), Am Ohrberg 1,  
D-31860 Emmerthal, Germany

\*\*SolarWerk GmbH, Iserstrasse 8-10, D-14153 Teltow, Germany

Received 3 August 1999; revised version accepted 14 April 2000

Communicated by VOLKER WITTWER

**Abstract**—Two different principles of thermoelectric cogeneration solar collectors have been realized and investigated. Concerning the first principle, the thermoelectric collector (TEC) delivers electricity indirectly by first producing heat and subsequently generating electricity by means of a thermoelectric generator. Concerning the second principle, the photovoltaic-hybrid collector (PVHC) uses photovoltaic cells, which are cooled by a liquid heat-transfer medium. The characteristics of both collector types are described. Simulation modules have been developed and implemented in TRNSYS 14.1 (1994), in order to simulate their behaviour in typical domestic hot-water systems. The discussion of the results shows that the electric output of the PV-hybrid collector is significantly higher than that of the thermoelectric collector. © 2000 Elsevier Science Ltd. All rights reserved.

### 1. INTRODUCTION

The aim of thermoelectric-hybrid solar collectors is to cogenerate thermal and electric energy within the same module. In cooperation with the company SolarWerk, Teltow (Germany), two different types of thermoelectric-hybrid collectors have been constructed and investigated at ISFH, according to their corresponding physical principles.

The first type is called a thermoelectric collector (TEC). The principle is to combine a solar thermal collector with a thermoelectric generator (TEG), which delivers the electric energy. The TEG is located between the absorber and the fluid pipe of the collector.

Thermoelectric energy conversion has been described in numerous publications. In most cases, the energy source has a high temperature, but applications in the range between 350 and 450 K are also discussed (Rowe *et al.*, 1995). In these cases, the heat source is, in general, very cheap and permanently available. A possible solar application reported by Rowe uses heat generated by a solar pond. The integration of a TEG into a non- or low-concentrating solar thermal collector is theoretically described by Chen (1996). However,

the example discussed by Chen is based on an extremely well-insulated flat plate collector, which, in practice, may be difficult to achieve.

The second collector type discussed in this paper is the photovoltaic-hybrid collector (PVHC). The idea of this collector is the combination of photovoltaic (PV) cells with a thermal collector. The PV cells are laminated on the surface of the solar absorber, which is cooled by a liquid heat-transfer medium.

PVHCs have been discussed in numerous publications for more than 20 years. One justification is to cool the solar cells in order to increase the electrical output. In many cases, this is done by air-cooled solar cells, which are mainly applied in integrated PV/thermal systems in buildings. The hot air is normally used for room-heating purposes (Cox and Raghuraman, 1985; Sopian *et al.*, 1996; Vandaele *et al.*, 1998).

A more effective cooling is necessary if the PV cells are arranged in a concentrating device like a CPC concentrator or a fresnel lens. In these cases, water instead of air is used as the heat-transfer medium (Kamoshida *et al.*, 1990; Rönnelid *et al.*, 1999). The preparation of hot water in the temperature range below 80°C has been evaluated at a small thermosyphon system by Garg *et al.* (1990) and at a 48 m<sup>2</sup> collector system in a single family house by Hayakashi *et al.* (1990). A PVHC absorber construction, which may be integrated into a building's structure, as an unglazed or

<sup>†</sup>Author to whom correspondence should be addressed. Tel.: +49-5151-999-521; fax: +49-5151-999-520; e-mail: ro.isfh@t-online.de

glazed element, is presented by Imre *et al.* (1993). Fujisawa and Tani (1997) have reported the construction and evaluation of two PVHCs with a single glass cover that show a thermal zero loss efficiency  $\eta_0$  of more than 0.7. A detailed theoretical and experimental study of water-cooled photovoltaic/thermal combined collectors has been carried out by de Vries (1998).

The theoretical description of PVHCs as water-cooled, single glazed, flat plate collectors is presented by several authors. Florschuetz (1979) derived the extension of the Hottel-Whillier equation for PVHCs, Bergene and Loevvik (1995) presented a detailed model for the collector's heat transfer. In order to assess the total energy gain of a PVHC system, Takashima *et al.* (1994) and Fujisawa and Tani (1997) proposed the use of the output energy for evaluation purposes.

This paper contains basic work for both collector types, the TEC and the PVHC. Collector prototypes have been constructed and evaluated experimentally. Furthermore, mathematical collector models have been developed and validated and, thus, system simulations could be carried out. The collector constructions and the main results of the investigations will be described.

## 2. THERMOELECTRIC COLLECTOR

### 2.1. Design principles and selected construction

The thermoelectric collector (TEC) combines a solar thermal collector with a thermoelectric generator (TEG). The TEG, which delivers the electric energy, is located between the absorber and the fluid pipe of the collector. Peltier elements, which are normally used for cooling purposes, may be specially designed for electricity generation and applied as TEG.

The thermal resistance of the TEG causes a temperature difference that is proportional to the heat flux from the absorber to the fluid. Furthermore, this temperature difference is proportional to the generated electric power. Thus, for a high electric performance, all solar thermal heat has to be conducted over the TEG. Therefore, a clear separation between the absorber and the fluid part of the collector is necessary, in order to concentrate the solar heat to one point, the hot junction of the TEG, and then to let it pass over the TEG to its cold junction.

This local concentration of heat may be obtained by a gravity-assisted heat-transfer process, like a boiling-condensing process in heat pipes or a thermosyphon cycle. For the following development, a water-filled heat pipe was used.

To generate a high amount of electric power, a high temperature difference at the TEG is necessary. This can only be achieved by a high thermal resistance of the TEG, which, consequently, leads to a high absorber temperature, if a significant amount of heat is led over the TEG. However, the high absorber temperature increases the thermal losses of the absorber and, therefore, reduces the solar heat production in the collector part. This results in a reduction of the thermal and electric gains. Therefore, it is necessary to use high temperature collectors, which requires at least evacuated tubular collectors (ETC), or, even better, ETC with concentrating mirrors. Fig. 1 shows a principle solution using an ETC with a heat pipe, which was investigated here.

Using a dry coupling, the condenser of the heat pipe heats the lower part of the heat exchanger to a high temperature. This part of the heat exchanger will act as the hot junction of the TEG. The upper part of the heat exchanger is cooled by the heat-transfer fluid, thus acting as the cold junction (see Fig. 1). The fluid is conducted to a consumer, e.g. to a system with a hot-water storage tank or an auxiliary heater. It may then be used for domestic hot-water preparation. The TEG is arranged between the hot and the cold junction. The heat passing the TEG creates electric power, which, at its maximum power point (MPP), is proportional to the temperature difference between the hot and cold junctions.

### 2.2. Investigations on thermoelectric generators

A central objective of the development work is to investigate the behaviour of appropriate TEGs with regard to their electric and thermal properties. For this purpose, a heat-exchanger test stand was built up and the behaviour of different TEGs [area around 9 cm<sup>2</sup>, thickness 3–5 mm, manufacturers Kunze (Deisenhofen, Germany)

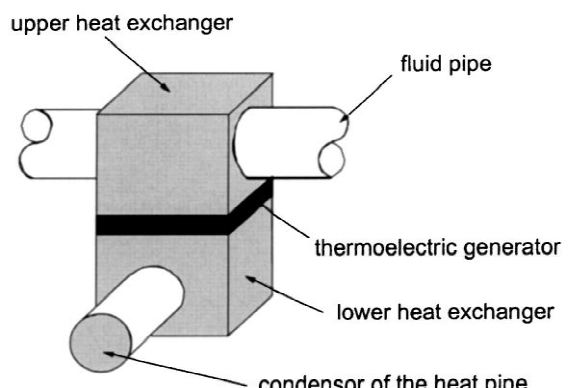


Fig. 1. Scheme of the thermoelectric collector.

and TECOM (Groebers, Germany)] was measured for varying boundary conditions (Giebel, 1997).

The interactions of the electric and thermal properties depend on various parameters, taking into account the different physical effects (mainly Seebeck- and Peltier-effects). For example, the electric output is a function of the mean TEG temperature, temperature difference and inner electric resistance of the element and is, therefore, coupled with the thermal resistance between the hot and cold junctions, which has been found to be dependent mainly on the mean temperature and the electric current generated by the element. Thus, both the thermal and the electrical characteristics depend on each other. A further complication is caused by the dependence of the inner electric resistance on the mechanical pressure to which the element is exposed by the heat-exchanger package. Finally, practical considerations like the heat-transfer resistance between the TEG and the heat exchanger, and the bypass heat flow caused by the clamping mechanism have also to be taken into account. For these reasons, only simplified dependencies could be developed here. The correlations, however, have been proved to be sufficiently precise for the description of the whole collector. A deviation between the measured and calculated results of less than  $\pm 3\%$  regarding the electric output was found during the investigations of the TEC collector prototype (under the test conditions, see Section 2.3).

For the behaviour of the electric output, the following simplified formula has been worked out:

$$P_{\text{el}} = \frac{R_{\text{load}}}{(R_i + R_{\text{load}})^2} \cdot [b_1 \cdot \Delta T_{\text{TEG}}^2 + b_2 \cdot \Delta T_{\text{TEG}}^2 \cdot T_{\text{avg}} + b_3 \cdot \Delta T_{\text{TEG}}^2 \cdot T_{\text{avg}}^2] \quad (1)$$

The heat transfer capability between the hot and cold junctions may be described by:

$$U_{\text{TEG}} = c_1 \cdot I + c_2 \cdot T_{\text{avg}} + c_3 \cdot I \cdot T_{\text{avg}} + c_4 \cdot I \cdot T_{\text{avg}}^2 + U_{\text{TEG0}} \quad (2)$$

It has been shown during the TEG experiments that both equations describe the measured behaviour with a high accuracy over the whole operation range (standard uncertainty of less than 8 and 7%, respectively).

The measured performance of the TEGs was at

an input heat of 60 W, with 20°C fluid temperature between 1.3 and 2.0 W, i.e. an efficiency of around 2.3 to 3.2% was achieved, while the TEG was operated in MPP. The thermal conductivity of one TEG is around 0.4 W/K, which causes a temperature difference between the hot and the cold junctions ( $\Delta T_{\text{TEG}}$ ) of around 150°C (in MPP-operation, irradiance level of approx. 900 W/m<sup>2</sup>).

### 2.3. Construction and assessment of the thermoelectric collector

A prototype of a thermoelectric collector was constructed. Three vacuum-tubes with heat pipes (producer Thermamax, UK), each with a 0.1-m<sup>2</sup> absorber area and with water as the heat-pipe medium, were connected via a specially designed heat exchanger to a fluid circuit. Fig. 2 shows the construction of one heat-exchanger element.

Special care was necessary in order to avoid additional thermal resistances between the heat exchanger and the junctions of the TEG. Furthermore, as only the heat passing via the TEG produces electricity, any bypass heat flow has to be minimized. This is important for the design and the selection of the clamp device and the surrounding insulation material. Finally, the temperature stability of the applied material has to be high enough to withstand the expected high temperature, especially in cases of stagnation.

The prototype collector was tested in agreement with ISO 9806-1 (1994). To assess the influence of the TEG's integration, a modified collector version without a TEG was also investigated. Due to the small amount of electric output, the thermal and electric yield may be discussed separately.

Fig. 3 shows the thermal efficiency curves of both versions of the collector.

The installation of the TEG, with its high thermal resistance, leads to a drastic decrease in the collector's efficiency factor and, thus, reduces

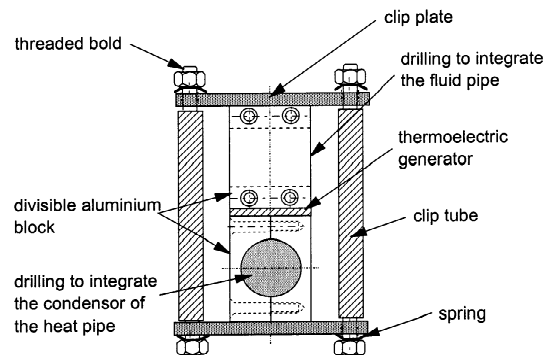


Fig. 2. Construction of the heat exchanger of the thermoelectric collector prototype.

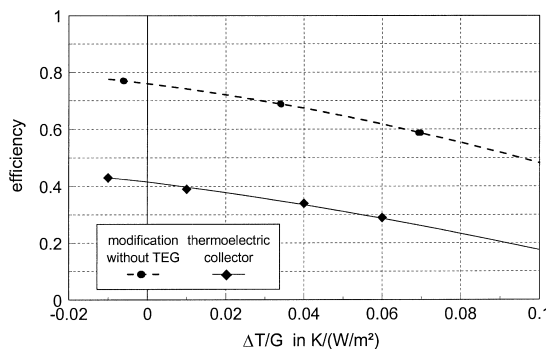


Fig. 3. Thermal efficiency curve of the thermoelectric collector, compared to same collector without a TEG. The irradiance level was approx.  $800 \text{ W/m}^2$ , the air speed was  $3 \text{ m/s}$  and the ambient air temperature was  $23^\circ\text{C}$ . Efficiency presentation with respect to aperture area and mean fluid temperature, according to ISO 9806-1 (1994).

the conversion factor  $\eta_0$  by around 45%, compared to an identical collector without a TEG. The electrical efficiency reached a maximum value of 1.1% of the incoming solar radiation, which is around 2.8% of the transferred heat. The electric efficiency decreases linearly from 1.1% at  $\Delta T/G = 0.0 \text{ Km}^2/\text{W}$  (i.e.  $T_{\text{amb}} = T_m = 23^\circ\text{C}$ ) to 0.65% at  $\Delta T/G = 0.05 \text{ Km}^2/\text{W}$  (i.e.  $T_{\text{amb}} = 23^\circ\text{C}$ ,  $T_m = 63^\circ\text{C}$ ,  $G = 800 \text{ W/m}^2$ ). In summary, the integration of a TEG raises the absorber temperature and this results in the losses of the solar collector being increased significantly, whereas the electric output remains rather small.

#### 2.4. Simulation of the thermoelectric collector and system

For the calculation of yearly energy gains, a dynamic simulation model was developed. As the thermal and electrical properties may not be isolated, an iterative calculation process is necessary. The model was validated with the experimental results of the prototype collector tests (Sillmann, 1997). The results were transferred to a TRNSYS simulation tool and, therefore, could be implemented in a solar system simulation programme.

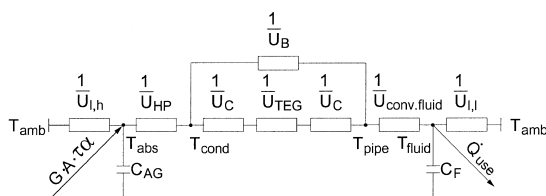


Fig. 4. Thermal model of the TEC.

Fig. 4 shows the thermal model of the TEC. First of all, annual simulations were carried out with a constant collector inlet temperature. The collector operates when its temperature is above the given fluid inlet temperature. The flow rate was kept constant ( $40 \text{ l/m}^2\text{h}$ ). The simulations lead to the following results:

- The thermal connection between the condenser and the TEG, and between the TEG and the fluid, must be good. A minimum heat-transfer capability between the absorber and the fluid of  $20 \text{ W/m}^2\text{K}$ , except for the TEG itself, should be achieved for the used vacuum tube, including the heat exchanger, with respect to the absorber area. The bypass heat flow should be minimized in order to achieve higher electric gains, whereas a higher bypass heat transfer increases the thermal output.
- With a constant inlet temperature of  $10^\circ\text{C}$ , a thermal output of  $660 \text{ kWh/m}^2$  and an electric output of  $14 \text{ kWh/m}^2$  may be expected per year at Hanover (Germany). At an inlet temperature of  $90^\circ\text{C}$ , the output is 260 respectively  $6 \text{ kWh/m}^2$  per year<sup>1</sup>.
- If a vacuum tube with a significantly lower loss coefficient compared to the prototype (stagnation temperature of around 70 K higher) was used, the thermal output would nearly be unaffected and the electric output would increase to  $15 \text{ kWh/m}^2\text{a}$  at  $10^\circ\text{C}$  and to  $10 \text{ kWh/m}^2\text{a}$  at a fluid inlet temperature of  $90^\circ\text{C}$ , which means that a better insulated collector primarily promotes the electric gains.
- An increase of the heat transfer capability,  $U_{\text{TEG}}$  of the TEG by a factor of two would increase the thermal output to  $750 \text{ kWh/m}^2\text{a}$  (at a constant fluid inlet temperature of  $10^\circ\text{C}$ ) and decrease the electric gain by approximately 50%. On the other hand, a reduction of the  $U_{\text{TEG}}$  by 75% would lower the thermal output to  $320 \text{ kWh/m}^2\text{a}$ , whereas the electric gain would rise to approx.  $40 \text{ kWh/m}^2\text{a}$ .
- A variation of the flow rate does not significantly affect the electric output of the collector, as this is mainly determined by the temperature difference between the absorber and the fluid. This temperature difference is essentially caused by the thermal resistance of the TEG, if all contact and bypass problems have been avoided. Therefore, a significant electric performance improvement cannot be

<sup>1</sup> 1 kWh = 3.6 MJ.

expected using a special flow-rate control strategy.

The prototype of the TEC has shown the technology's inherent disadvantage, i.e. that the high thermal performance of evacuated tubular collectors will be significantly decreased and the returned electric energy is relatively small. Therefore, the conversion efficiency of the TEG has to be improved. The best laboratory elements attain efficiency values that are about three-times higher than the elements used. They attain around 30% of the Carnot efficiency (Rowe *et al.*, 1995), which is assumed to be at the upper technical limit, which means an efficiency increase of the TEG by a factor of three, if compared to those TEGs used in the prototypes. This theoretical improvement in the TEG would not significantly influence the thermal output of the improved thermoelectric collector<sup>2</sup>, but it would increase the electric gain by a factor of 2.5, if the improved TEC was operated with a constant fluid inlet temperature (10°C) over one year.

With these improved elements, annual simulations of a typical solar domestic hot-water system were carried out. The solar system consists of a 5 m<sup>2</sup> TEC, with an inclination angle of 35°, south, is located in Hanover, Germany, and is connected via an internal heat exchanger to a 350-l drinking-water storage system. The hot-water demand is 165 l/day at a demand temperature of 45°C (2600 kWh/a). The collector flow-rate is 200 l/h, which is controlled by a temperature-difference control-

ler (pump on: collector temperature more than 10 K above the storage temperature; pump off: collector temperature less than 2 K above the storage temperature) (Sillmann, 1997). The heat-transfer capability of the TEG was varied during the system simulations. Fig. 5 shows how the variation of the conductance affects the electric and thermal energy outputs.

If 5 m<sup>2</sup> of the constructed prototype collector, equipped with the improved TEG, was installed in the typical hot-water system described above, a yearly gain of 1650 kWh of thermal and of 50 kWh of electric energy could be achieved. Fig. 5 shows that a lower TEG conductivity increases the electric gain, but strongly reduces the thermal gain. If the conductivity is halved, the yearly electric output is nearly doubled, to 100 kWh/a, whereas the thermal gain is reduced by around 500 kWh/a (i.e. 30%).

The same thermal collector output of 1650 kWh/a would be achieved with the standard vacuum tube collector (without the TEG) with a collector area of 3.1 m<sup>2</sup>, which means that nearly 2 m<sup>2</sup> of the collector are necessary to compensate for the additional collector losses caused by the TEG.

The discussion shows that a thermoelectric collector with acceptable technical properties needs highly efficient vacuum collectors and highly efficient TEGs, both at the upper technical limit. However, even with these components, it seems to be unrealistic to develop a thermoelectric collector with economically promising prospects. Even if the cost share for the TEGs and their integration is neglected, the additional area of 2 m<sup>2</sup> of the evacuated tubular collector in the example presented only results in a 50-kWh/a electric gain. At a price of 500 \$/m<sup>2</sup> for this additional area, the investment costs are 20 \$/(kWh/a). This is significantly higher than electricity production using photovoltaic modules [below 8 \$/(kWh/a)]. A realistic cost estimation for the TEGs, including their integration, is not possible at the moment. However, if one could take these costs into account, the amount of investment per kWh/a would increase significantly.

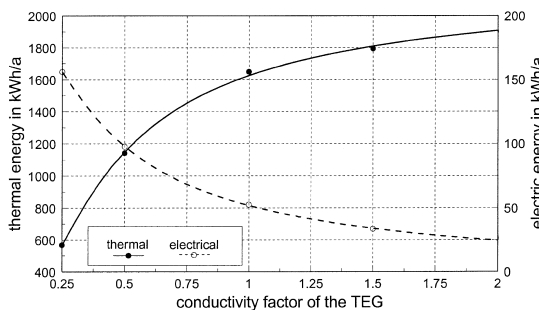


Fig. 5. Annual energy yield of a thermoelectric collector with an efficiency-improved TEG in a solar domestic hot-water system (Hanover) vs. conductivity factor of the TEG. The conductivity factor is a multiple of the measured heat-transfer capability of the prototype (collector area, 5 m<sup>2</sup>; energy demand, 2600 kWh/a).

<sup>2</sup>The improved TEC is a theoretical collector combination, in which the improved TEGs, with a conversion efficiency that was three-times higher, were applied together with the vacuum tubes of the prototype.

### 3. PHOTOVOLTAIC-HYBRID COLLECTOR

#### 3.1. Design principles of a photovoltaic-hybrid collector

A photovoltaic-hybrid collector (PVHC) results

from the combination of photovoltaic (PV) cells with a thermal flat plate collector. The PV cells are laminated onto the surface of an aluminium solar absorber. On its back side, a copper fluid pipe is clamped on. This PVHC absorber is cooled by a liquid heat-transfer medium. The absorber is integrated in a standard aluminium frame with normal solar glass, an air gap of 3 cm and a backside insulation (mineral wool) of 5 cm. Fig. 6 shows the explosion drawing of the PVHC.

A small thermal resistance between the PV cells and the fluid is important for the effectiveness of the PVHC. Both the thermal and the electric performance decrease with rising fluid temperature. The absorber temperature is strongly affected by the fluid temperature. As the fluid inlet temperature typically depends on the design and operation of the complete solar hot-water system, especially on the ratio of solar gain to hot-water demand, the system parameters are very important too. This will be shown in the following.

### 3.2. Collector model

In order to support the development work, a simulation model was necessary. The model was used for component optimization and for the simulation of a whole solar system. To use the universal properties of TRNSYS, the PVH collector module was written as a TRNSYS-type and implemented into a TRNSYS configuration of a solar domestic hot-water system. The PVH collector model has to describe both the electric and the

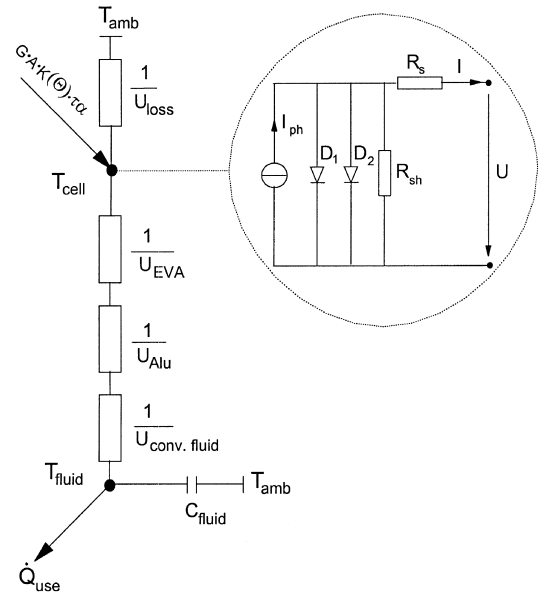


Fig. 7. Thermal and electrical model for the PVHC.

thermal behaviour, as well as the interaction between these characteristics.

Fig. 7 shows the node model as a basis for the thermal considerations, including the integrated 'two-diode'-model for the description of the electric performance of the PV cells. The interaction between both models is taken into account by the cell temperature, which on the one hand, affects the cell's performance and, on the other hand, is almost equivalent to the absorber tem-

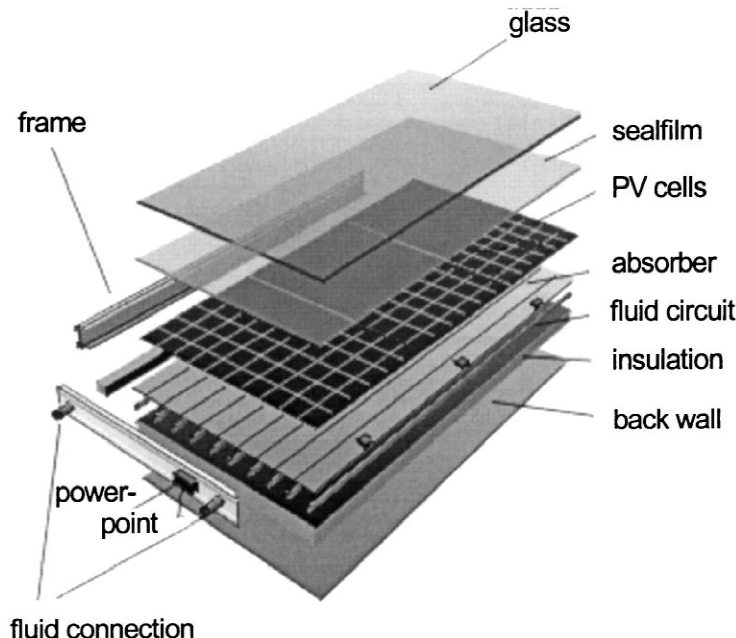


Fig. 6. Construction of the photovoltaic-hybrid collector (PVHC).

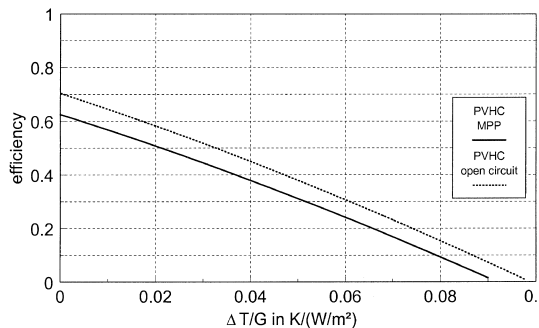


Fig. 8. Thermal efficiency curves of the PVH collector, with maximum electric efficiency (MPP) and in open-circuit mode. Efficiency presentation with respect to mean fluid temperature and aperture area, according to ISO 9806-1 (1994).

perature and, therefore, directly influences the thermal gain and loss mechanisms.

This model has been developed interactively with the experiments performed with the first prototypes. The development process has shown that it is sufficient to introduce only one thermal capacitance into the model, located in the fluid node. This inaccuracy is acceptable as the thermal resistance between the fluid and the cell node is rather low (this has not been the case at the TEC, compare with Section 2).

The validation procedure of the final simulation programme shows good agreement with the measured data, even in the dynamic parts of the time series.

### 3.3. Performance of the PV-hybrid collector

The general thermal behaviour is similar to that of a nonselective flat plate collector. The reason is the high thermal emissivity of the laminate-cell-package ( $\varepsilon$  of around 0.90), which leads to a high thermal loss coefficient. The conversion factor  $\eta_0$  of the PVH collector is only somewhat smaller than  $\eta_0$  of a nonselective flat plate collector. The difference is caused by the absorption coefficient,  $\alpha$ , which reaches 0.91. This is a few percentage points lower than that obtained with a black solar colour. The electrical operation mode has to be

taken into account. If the PV-part is operated in open respectively short circuit, i.e. no electric power is drawn off, the heat generation will be higher compared to that obtained at maximum power point (MPP) operation.

The efficiency curves were measured at an irradiance level of about  $820 \text{ W/m}^2$  and at an ambient air speed of 3 m/s. Fig. 8 shows that the thermal efficiency curve, presenting the electric MPP-operation, is moved downwards, almost in parallel, by around 0.10 if compared to the open-circuit curve. That means that the extraction of electric energy directly affects the zero loss efficiency,  $\eta_0$ , but has little effect on the heat loss coefficient. Consequently, the stagnation temperature of a PVH collector decreases if the electric part is operated at the MPP-point (see below).

The thermal parameters were determined according to ISO 9806-1 (1994), with the mean fluid temperature as the reference temperature and the aperture area ( $2.1 \text{ m}^2$ ) as the reference area. The electric performance indicators are the aperture-area-related and the cell-area-related efficiency data, the electric power of the module (cell area  $1.81 \text{ m}^2$ ), the open-circuit voltage and the short-circuit current, which were all referred to as standard test conditions (STC, irradiance,  $1000 \text{ W/m}^2$ ; cell temperature,  $25^\circ\text{C}$ ).

Table 1 shows that the difference between the conversion factors,  $\eta_0$ , in either MPP or open circuit, is nearly equivalent to the electrical MPP-efficiency, what is a nice approval for the first law of thermodynamics in this special case. During the efficiency measurements with a low inlet temperature, the mean cell temperature was only 11 K above the fluid temperature.

For the implementation of the simulation programme, more detailed parameters than the ISO-coefficients and STC-parameters are required. For this purpose, the parameters of the electric two-diode-model were identified, as were the single thermal resistances between the cell node and either the fluid or the environment node, as displayed in Fig. 7.

Table 1. Performance parameters of the PVH collector prototype (aperture area,  $2.1 \text{ m}^2$ ; cell area,  $1.8 \text{ m}^2$ )

Thermal coefficients		Electrical coefficients (STC)	
$\eta_0$ [–]	0.726 (PV-open circuit) 0.633 (PV-MPP)	$I_{sc}$ [A]	2.84
$a_1$ [ $\text{W/m}^2\text{K}$ ]	5.88 (PV-open circuit) 5.64 (PV-MPP)	$U_{oc}$ [V]	107
$a_2$ [ $\text{W/m}^2\text{K}^2$ ]	0.016 (PV-open circuit) 0.015 (PV-MPP)	$P_{MPP}$ [W]	220
		$\eta_{el}$ [–]	0.103 (aperture area) 0.121 (cell area)

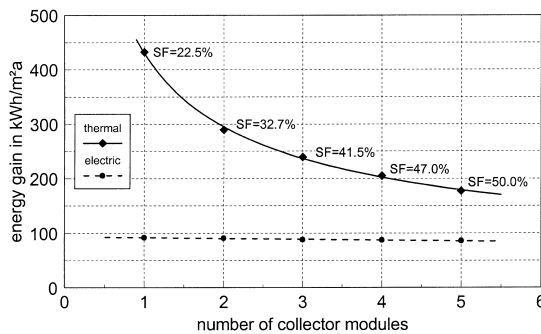


Fig. 9. Annual thermal and electric energy gain versus the number of PVHC-modules, with additional data on the solar fraction of the hot-water demand (SF).

### 3.4. Simulation of the PVHC system yield

As the basis for the system simulations, the same solar system as discussed in Section 2.4 was used. The system comprised a domestic hot-water system with collector modules arranged in series, a single drinking-water storage system, an internal heat exchanger, and was simulated using weather data (TRY) for Würzburg, Germany, with an inclination angle of 35°, south. The annual heat demand was 2600 kWh/a at a demand temperature of 45°C. The collector was increased from one module (2.1 m<sup>2</sup>), in steps, up to five modules. Fig. 9 shows the results of these simulations.

While the thermal gain decreases from 432 to 177 kWh/m<sup>2</sup>a, the electric gain only decreases from 92 to 86 kWh/m<sup>2</sup>a. The solar fraction of the thermal demand increases from 22% (with one module) to 50% with five modules. As the collector has a thermal performance like that of a nonselective flat plate collector with additionally reduced thermal gains, the system output in central Europe is restricted to a solar fraction of around 50%. This means that significantly higher solar fractions, corresponding to a 100% coverage of the demand during the summer, may hardly be achieved. Ideally, this collector should be used in preheating systems where both the thermal and the electric gains can benefit from the low fluid-inlet temperature.

In order to attain a higher solar fraction,

installation of a series of PVH collector modules and standard selective flat plate collector modules is possible. Table 2 shows the annual output of different combinations. The combination of PVH collector modules and selective flat plate collector modules leads to higher solar fraction values. However, the thermal system should be designed such that long periods of stagnation, which lower the PV yield, are avoided.

The electric output of the PVH collector is somewhat lower than that of standard PV modules, which would reach an annual yield of about 100 to 110 kWh/m<sup>2</sup>. This difference is caused mainly by the higher reflection losses at the glass pane and a relatively low ratio of cell and aperture area. At the PVHC, this ratio is 0.85, whereas it is around 0.90 for standard PV modules. If the annual yield is related to the peak electric power (instead of module area), the electric output of the PVH collector is nearly identical to that of standard PV modules. The influence of the module temperature is rather small, which will be discussed.

As the efficiency of the PV cells rises with decreasing temperatures, low module temperatures are desired. One of the main questions concerning PV-hybrid systems is whether or not the mean operation temperature is higher compared to standard PV modules. For this purpose, the irradiation weighted mean cell temperature is defined as follows:

$$\overline{T_{\text{cell}}} = \int (G \cdot T_{\text{cell}}) dt / \int G dt \quad (3)$$

For standard PV modules, the weighted mean cell temperature mainly depends on wind exposure and the integration technique. For typical PV modules mounted on a roof in Germany, with a backside ventilation layer, an energetically weighted mean cell temperature of between 28 and 40°C may be derived from the results of the German '1000-Dächer-Programm' (Kiefer and Hoffmann, 1997). If the PV modules are integrated in a roof construction, with reduced backside air ventilation, an additional increase of the

Table 2. Annual output of PVHC and selective flat plate collector (FPC) and solar fraction, for different module combinations (2.1 m<sup>2</sup> collector area for each module)

	2 PVHC & 1 FPC	2 PVHC & 2 FPC	4 PVHC & 1 FPC
PVHC <sub>th</sub> [kWh/m <sup>2</sup> ]	291	232	193
FPC <sub>th</sub> [kWh/m <sup>2</sup> ]	399	310	352
PVHC <sub>el</sub> [kWh/m <sup>2</sup> ]	90.8	88.5	87.0
SF [-]	0.53	0.60	0.60

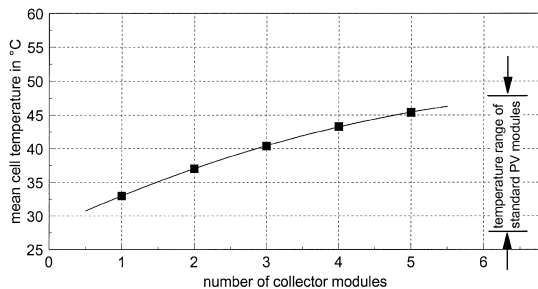


Fig. 10. Irradiation weighted mean cell temperature of the PVHC versus number of collector modules, in comparison to standard PV modules.

cell temperature by around 8 K may be assumed (Krauter, 1993). Thus, the energetically weighted mean cell temperature of standard PV modules in Germany is in the range between 28 and 48°C. Fig. 10 shows that the mean cell temperature of the PVHC increases with increasing number of modules, from 33°C to 45°C. However, even with five modules ( $10.5\text{ m}^2$ ), it is still in the range of standard PV modules. In a warmer climate, as in southern Europe, where the mean cell temperature of standard PV modules is higher, the energetically weighted PVHC temperature could even be lower than that of standard PV modules.

### 3.5. Reliability questions and the potential for improvement

The PVHC reaches a stagnation temperature of 147°C at  $1000\text{ W/m}^2$ , at an ambient temperature of 30°C and in calm wind conditions, if operated under open-circuit conditions. This is a typical value for nonselective collectors. If the module is operated at the same time at its electrical maximum power point, the stagnation temperature decreases by around 12°C. Special regard must be given to the laminate construction, the electric cables and the connecting boxes, which all have to withstand these extreme temperatures.

The collector prototype already exhibits a good performance, which has little potential for improvement with this construction type. The thermal contact between the absorber and the fluid may still be improved slightly, which may lead to an increase in the thermal gain of about 2 to 4%. New, high-efficiency cells could lead to an enhancement of the electric gain.

## 4. CONCLUSIONS

The principle of the TEC is to produce first

heat, and then to transfer this heat over the thermal resistance of the TEG, where it will partly be transformed into electricity, with the remaining heat having to be cooled. It follows from this serial energy flow that the absorber must be maintained at a high temperature, as the electrical generator needs a high temperature difference. Therefore, even with high-efficiency collectors, the thermal efficiency will decrease significantly. One important requirement is to use solar collectors with very low loss coefficients, e.g. by concentrating the irradiance. A further disadvantage is the low conversion factor of TEGs, where only 30% of the Carnot efficiency seems to be realistic.

In contrast to the TEC, the principle of the PVH collector is the direct production of electricity, i.e. the efficient, direct use of the high-energy content of the radiation, and only the remaining radiation energy is transformed to heat. This heat will be used on a temperature level as requested by the thermal part of the solar system. Hence, the PVH collector produces heat and electricity in parallel.

Comparison of the solar system simulations between the existing PVH collector prototype and the advanced extrapolated TEC shows the advantage of the PVHC principle. The improved TEC ( $5\text{ m}^2$  evacuated tubular collector) would lead to an electricity gain of 50 kWh/a and meet the thermal demand with a solar fraction of 53%. The PVHC ( $10.5\text{ m}^2$ ) delivers around 920 kWh/a electric energy and covers the thermal demand by 50%. Regarding the same collector area of  $5\text{ m}^2$ , the PVH collector produces 450 kWh/a of electricity, which is nine-times higher than the electricity production of the advanced extrapolated TEC.

Precise cost statements or estimations are not available. It may, however, be assumed that the production technology of the PVH collector, with its known processes from PV module and thermal flat plate collector techniques, has a higher economic potential.

Therefore, it may be concluded that the TEC will only be of interest for special applications. In a direct comparison, PVH collector technology shows many advantages. However, hybrid collectors often show non-optimum behaviour in comparison to the parallel operation of the separate technologies. However, for specific applications and special purposes, the advantages of only one type of solar module for heat and electricity production may be so convincing that it is our

opinion that these collectors will occupy a place in future developments and future markets.

## NOMENCLATURE

$A$	area ( $\text{m}^2$ )
$a_1$	collector coefficient according to ISO 9806-1, representing the constant part of the collector heat losses, with respect to $T_m$ ( $\text{W}/\text{m}^2\text{K}$ )
$a_2$	collector coefficient according to ISO 9806-1, representing the temperature-dependent part of the collector heat losses, with respect to $T_m$ ( $\text{W}/\text{m}^2\text{K}^2$ )
$b_1, b_2, b_3$	coefficients to calculate the electric energy gain of the TEG (different dimensions)
$c_1, c_2, c_3, c_4$	coefficients to calculate the heat-transfer capability of the TEG (different dimensions)
$C_{AG}$	capacity portion of the TEC, with respect to the absorber temperature ( $\text{kJ}/\text{K}$ )
$C_F$	capacity portion of the TEC, with respect to the fluid temperature ( $\text{kJ}/\text{K}$ )
$C_{\text{fluid}}$	capacity of the PVHC, with respect to the fluid temperature ( $\text{kJ}/\text{K}$ )
$D_1, D_2$	diodes of the two-diode-model
$G$	global solar irradiance, measured in collector plane ( $\text{W}/\text{m}^2$ )
$I$	current (A)
$I_{\text{ph}}$	photo-current (A)
$I_{\text{sc}}$	short circuit current (A)
$K$	incident angle modifier coefficient (-)
$P_{\text{el}}$	electric power (W)
$P_{\text{MPP}}$	electric power in MPP operation (W) useable heat-flux, transported with the fluid (W)
$R_i$	inner resistance ( $\Omega$ )
$R_{\text{load}}$	load resistance ( $\Omega$ )
$R_s$	serial resistance of the two-diode-model ( $\Omega$ )
$R_{\text{sh}}$	shunt resistance of the two-diode-model ( $\Omega$ )
$t$	time (s)
$T_{\text{abs}}$	absorber temperature ( $^{\circ}\text{C}$ )
$T_{\text{amb}}$	temperature of the ambient air ( $^{\circ}\text{C}$ )
$T_{\text{avg}}$	average temperature of the TEG ( $^{\circ}\text{C}$ )
$T_{\text{cell}}$	temperature of the PV cells ( $^{\circ}\text{C}$ )
$T_{\text{cond}}$	temperature of the condensor of the heat pipe of the TEC ( $^{\circ}\text{C}$ )
$T_{\text{fluid}}$	temperature of the heat-transfer fluid ( $^{\circ}\text{C}$ )
$T_m$	arithmetical mean temperature of the heat-transfer fluid inlet and outlet temperatures ( $^{\circ}\text{C}$ )
$T_{\text{pipe}}$	temperature of the fluid pipe of the TEC ( $^{\circ}\text{C}$ )
$\Delta T$	temperature difference between mean fluid temperature and ambient air temperature (K)
$\Delta T_{\text{TEG}}$	temperature difference between the hot junction and the cold junction of the TEG (K)
$SF$	solar fraction (-)
$U$	voltage (V)
$U_{\text{oc}}$	open circuit voltage (V)
$U_B$	heat-transfer capability of the bypass of the TEC, with respect to collector area ( $\text{W}/\text{m}^2\text{K}$ )
$U_{\text{Alu}}$	heat-transfer capability of the aluminium absorber, with respect to collector area ( $\text{W}/\text{m}^2\text{K}$ )
$U_C$	heat transfer capability between the TEG and the aluminium block of the TEC, with respect to collector area ( $\text{W}/\text{m}^2\text{K}$ )
$U_{\text{conv.fluid}}$	heat-transfer capability between the fluid pipe and the fluid, with respect to collector area ( $\text{W}/\text{m}^2\text{K}$ )
$U_{\text{EVA}}$	heat-transfer capability of the laminate, with respect to collector area ( $\text{W}/\text{m}^2\text{K}$ )
$U_{\text{HP}}$	heat-transfer capability of the heat pipe of the
$U_{\text{loss}}$	TEC, between the absorber and condensor, with respect to collector area ( $\text{W}/\text{m}^2\text{K}$ )
$U_{l,h}$	effective heat-loss coefficient between the absorber and ambient air, with respect to collector area ( $\text{W}/\text{m}^2\text{K}$ )
$U_{l,l}$	heat-transfer capability between the absorber of the TEC and ambient air, with respect to collector area ( $\text{W}/\text{m}^2\text{K}$ )
$U_{\text{TEG}}$	heat-transfer capability between the fluid of the TEC and ambient air, with respect to collector area ( $\text{W}/\text{m}^2\text{K}$ )
$U_{\text{TEG0}}$	heat-transfer capability of the TEG between the hot and cold junctions ( $\text{W}/\text{K}$ )
$\alpha$	absorption coefficient of the absorber layer (-)
$\varepsilon$	emissivity of the absorber layer, for infrared radiation above 4 $\mu\text{m}$ wavelength (-)
$\eta_0$	conversion factor; i.e. thermal collector efficiency at $\Delta T=0$ , with respect to $T_m$ (-)
$\eta_{\text{el}}$	electrical efficiency (-)
$\Theta$	incident angle ( $^{\circ}$ )
$\tau\alpha$	effective transmission-absorption product (-)

## REFERENCES

Rowe D. M. *et al.* (1995). *CRC Handbook of Thermoelectrics*, CRC Press, Boca Raton, FL.

Chen J. (1996) Thermodynamic analysis of a solar-driven thermoelectric generator. *J. Appl. Phys.* **79**(5), 2717–2721.

Cox C. H. and Raghuraman P. (1985) Design considerations for flat-plate-photovoltaic/thermal collectors. *Solar Energy* **35**(3), 227–241.

Sopian K. *et al.* (1996) Performance analysis of photovoltaic thermal air heaters. *Energy Conversion and Management* **37**(11), 1657–1670.

Vandaele L., Wouters P., Bloem J. J. and Zaaiman W. J. (1998) Combined heat and power from hybrid photovoltaic building integrated components: Results from overall performance assessment. *Proceedings of 2nd World Conference on Photovoltaic Solar Energy Conversion* **3**, 2698–2701.

Kamoshida J., Isshiki N. and Katayama K. (1990) Optical/thermal design and simulation of fixed line focus fresnel concentrator for combined photovoltaic-thermal applications. *Proc. 1991 Congr. ISES* **1**, 374–378.

Rönnelid M., Perers B., Karlsson B. and Krohn P. Cooling of PV modules equipped with low-concentrating CPC reflectors. *Proc. 1999 ISES Solar World Congress*. In press.

Garg H. P., Bhargava A. K. and Agarwal R. K. (1990) Experimental and theoretical studies on a photovoltaic/thermal hybrid solar collector water heater. *Proc. 1991 Congr. ISES* **1**, 701–705.

Hayakashi B., Mizusaki K., Satoh T. and Hatanaka T. (1990) Research and development of photovoltaic/thermal hybrid solar power generation system. *Proc. 1991 Congr. ISES* **1**, 302–306.

Imre L., Bitai A., Boehoency F., Hecker G. and Palfi M. (1993) PV-thermal combined building elements. *Proc. ISES Solar World Congr. 1993* **3**, 277–280.

Fujisawa T. and Tani T. (1997) Binary utilization of solar energy with photovoltaic thermal hybrid collector. *Proc. ISES Solar World Congr. 1997* **2**, 559–564.

de Vries D. W. (1998). *Design of a Photovoltaic/thermal Combi-panel*, Eindhoven University Press, Eindhoven.

Florschuetz L. W. (1979) Extension of the Hottel-Whillier model to the analysis of combined photovoltaic/thermal flat plate collectors. *Solar Energy* **22**, 361–366.

Bergene T. and Loevik O. M. (1995) Model calculations on a flat-plate solar heat collector with integrated solar cells. *Solar Energy* **55**(6), 453–462.

Takashima T. et al. (1994) New proposal for photovoltaic-thermal solar energy utilization method. *Solar Energy* **52**(3), 241–245.

Giebel, U. (1997) Untersuchungen an thermoelektrischen Elementen zur Stromerzeugung in Sonnenkollektoren. Diploma thesis at Institut für Solarenergieforschung, Emmerthal, Germany.

Sillmann, R. (1997) Konstruktion, meßtechnische Bewertung und Simulation eines thermoelektrischen Kollektors. Diploma thesis at Institut für Solarenergieforschung, Emmerthal, Germany.

TRNSYS 14.1. *A Transient System Simulation Program*, Solar Energy Laboratory, University of Wisconsin, Madison.

ISO 9806-1 (1994). *ISO Standard 9806-1: Test Methods for Solar Collectors. Part 1: Thermal Performance of Liquid Heating Collectors Including Pressure Drop*, ISO, Switzerland.

Kiefer K. and Hoffmann V. U. (1997). *1000-Dächer Meß- und Auswerteprogramm Jahresjournal 1996*, Fraunhofer Institut für Solare Energiesysteme ISE, Freiburg.

Krauter S. (1993). *Betriebsmodell der optischen, thermischen und elektrischen Parameter von photovoltaischen Modulen*, Köster, Berlin.